Berliner Beiträge zur Archäometrie, Kunsttechnologie und Konservierungswissenschaft

Rathgen-Forschungslabor
Staatliche Museen zu Berlin

24/2016

Berliner Beiträge zur Archäometrie, Kunsttechnologie und Konservierungswissenschaft

Band 24

Berlin 2016

Rathgen-Forschungslabor
Staatliche Museen zu Berlin

Herausgeberin:

Dr. habil. Ina Reiche
Rathgen-Forschungslabor, Staatliche Museen zu Berlin –
Preußischer Kulturbesitz
Schloßstraße 1a
14059 Berlin

Redaktionsassistentin:

Sabrina Buchhorn
Rathgen-Forschungslabor, Staatliche Museen zu Berlin –
Preußischer Kulturbesitz

© 2016 Staatliche Museen zu Berlin –
Preußischer Kulturbesitz

www.smb.museum

Herstellung:

Ruksaldruck GmbH und Co. KG Repro plus Offset
Lankwitzer Straße 35
12107 Berlin
Printed in Germany

Titelbild: Bemalung einer Museumsreplik der Nofretete © Staatliche Museen zu Berlin,
Gipsformerei / Foto: Jürgen Hohmuth; NCS Farbkreis ©dtp studio oldenburg

ISSN: 0344-5089

Inhalt

Vom Original zum Malmodell: Die Bemalung der neuen Replik der Nofretete-Büste der Gipsformerei, Staatliche Museen zu Berlin
THOMAS SCHELPER et al. 9

Seriation und Clusteranalyse von Objekten mit binären Merkmalen, erläutert am Beispiel von Götterdarstellungen des Löwentempels von Musawwarat es Sufra (Sudan)
HANS-GEORG BARTEL und HANS-JOACHIM MUCHA 21

First physico-chemical *in situ* investigations on the Lienzo Seler II of Coixtlahuaca
SILVIA MARTEN et al. 39

***In situ* scientific analyses of the leather wall hanging "Ilha Formosa"**
CRISTINA LOPES AIBÉO et al. 55

Zur Maltechnik von Otto Freundlich (1878-1943). Maltechnische und materialanalytische Untersuchungen am Beispiel des Spätwerks
VERENA FRANKEN et al. 69

Micro-fading testing on modern ink based pens and contemporary drawings from the Kupferstichkabinett Berlin
CARLOS MORALES-MERINO et al. 89

Die Skulpturen des Triumphkreuzes der Naumburger Moritzkirche – Untersuchungen zur Restaurierungsgeschichte und Kunsttechnologie, Teil 2
DIETER KÖCHER 103

An incense holder decorated with *émail champlevé*: a non-invasive multi-technical micro-analytical study
GAIA FENOGLIO et al. 129

Goldschmiedetechnische und materialanalytische Untersuchungen des sogenannten „Giselaschmucks"
JOCHEM WOLTERS 141

An incense holder decorated with *émail champlevé*: a non-invasive multi-technical micro-analytical study

Gaia Fenoglio[1], Stefan Röhrs[2], Lothar Lambacher[3], Ina Reiche[2]

[1]Dept. of Chemistry, University of Torino, Torino, Italy
[2]Rathgen-Forschungslabor, Staatliche Museen zu Berlin – Preußischer Kulturbesitz
[3]Kunstgewerbemuseum, Staatliche Museen zu Berlin – Preußischer Kulturbesitz

Abstract

An incense holder decorated with *émail champlevé* was analysed in a non-invasive way by two micro-analytical techniques. The appearance of the enamel in colour and structure raised doubts about the originality of the enamelled areas. Micro X-ray fluorescence and micro-Raman spectroscopy have been used to characterise the enamel as well as the metal and the gilding. While the analysis of the metal and gilding did not indicate any particular compositional features that contradict the medieval origin of the object, the analysis of the enamel suggested a post-medieval material.

Archival documentation on the incense holder implies that the object has received a re-enamelling at some point in its history before 1856 when it came into the collection of the Königliche Kunstkammer in Berlin.

1 Introduction

The collection of the *Kunstgewerbemuseum* (KGM) der Staatlichen Museen zu Berlin holds a so called *Weihrauchschiffchen* which is a liturgical boat-shaped incense holder. This incense holder with a circular foot has a flat lid which can be opened on one side and is made from gilded copper of which large parts are decorated with opaque *émail champlevé* (Inv. Nr. K 4195; height 5.3 cm, length 17.9 cm, width 8.8 cm, Fig. 1).

On the lid, surrounding two inset cabochons and their floral ornamental engravings, uniform dark blue enamel has been applied encircled by a narrow frame of opaque turquoise enamel.

The boat-shaped body of the incense holder is decorated with an engraved waved band framed with dark blue and red enamel between two bands of a rectangular pattern in turquoise enamel.

The Berlin *Weihrauchschiffchen* has been unanimous addresses as a Limoges work from the early 13th century (Braun 1932, Kötzsche 1975) and has been incoporated into the second volume of the *Corpus des émaux méridionaux* (CEM II, VI C, n° 1) (Gauthier et al. 2011) as '*Limoges, vers 1210-1215*' in 2011.

During a recent campaign of analysis performed on medieval enamels of the *Kunstgewerbemuseum* (KGM), the visual inspection of this specific object raised doubts about the originality of the enamelled areas. The peculiar hue of the blue enamel and, in particular, the very homogenous colour and opacification of the enamel - suggesting the use of industrial finely ground powder (Biron et al. 1996) - could indicate a modern production of the artwork or at least, a re-enameling, in the 19th or early 20th century. On the insert in Fig 1. it can be seen that the red enamel is laying over a more greenish material. This unusual type of layering also represents a technological peculiarity. The re-enamelling, whose resulting artefacts are called *pastiches* or *mariages*, is a well-known procedure both in ancient and modern times (Richter 1994, Wypyski 2000) and can involve parts or the total of the enamelled areas.

The analysis of incense holder K 4195 intended to analyse those areas which were suspected to be made with modern materials by a non-invasive multi-techniques approach based on optical microscopy, colour measurements, micro-X-ray fluorescence (μXRF) and micro-Raman spectroscopy.

Colour measurements were made to capture the peculiar hue of the blue enamels and to compare the colour with previous measured colours of medieval émaux *champlevé*. XRF analysis was performed to evaluate whether the composition of the enamels was compatible or not with an original medieval Limoges enamel, the results being compared with previous literature (Freestone 1991, Biron et al. 1996, Röhrs and Stege 2004, Agostino et al. 2010, Biron 2015). The presence of compositional markers characteristic of historical enamel productions generally makes possible a subdivision between medieval Limoges artworks and later "in style of Limoges" artefacts, the last being easily recognised by the use of lead arsenate as opacifier.

Raman spectroscopy was applied to confirm colorants and opacifiers propositions made upon XRF results and to characterise the matrix of the analysed glassy materials.

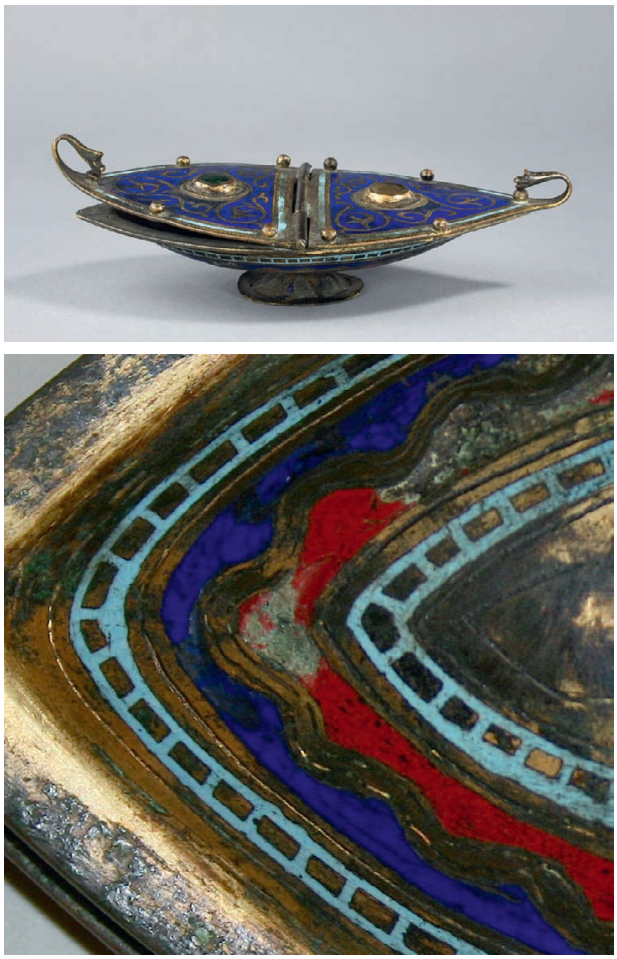

Fig. 1: Above: Incense holder K 4195 from the *Kunstgewerbemuseum*, Staatliche Museen zu Berlin – Preußischer Kulturbesitz. Below: The image shows the view from below.

2 Experimental

2.1 Micro-X-ray fluorescence

Micro-XRF analysis was performed at the Rathgen-Forschungslabor using a Bruker ARTAX spectrometer equipped with a Mo target and SDD detector. Measurements were collected using the following setup: 45 kV voltage, 500 µA current, 100 s accumulation time, He flux, no filter. The working distance was about 1 mm and the spot size about 100 µm. The instrument has an XYZ motorized head and a camera-laser system for sample positioning.

Spectra processing was performed using WinAxil Software from IAEA (Van Espen and Lemberge 2000) and quantitative data was obtained with WinFund module using standard materials. These included Corning reference glasses (A, B, C and D), produced to be used in historical glass studies (Brill 1999, Wagner et al. 2012), two soda-lime glasses (NSM 610, SGT11) and two Pb-bearing standards (CRM-CZ-400 and SRM 89). Considering the presence of different typologies of glass matrix, the standards to be used in the calibration were carefully chosen to properly predict matrix effects.

2.2 Micro-Raman spectroscopy

Micro-Raman Spectroscopy was performed using a Horiba XploRa Micro-Raman system. Spectra were acquired using a 532 nm laser with maximum power of 25 mW, 500 hole, 100 slit, 1800 lines/mm grating. The typical measuring time and number of accumulation was 5 times 5-25 s for crystalline phases characterization and 5 times 25 s for the glass matrix. Analyses were performed using a horizontal laser beam arrangement that allows measuring large objects, which do not fit on the traditional microscope sample stage. The modified arrangement consists in a 45° inclined mirror placed in the laser pathway, and a short tube (80 mm) placed between the mirror and the objective. A 10x or a 50x LWD (Long working distance) microscope objective was chosen according to measures necessities; the 50x LWD was the one typically used. In order to control the sample positioning towards the horizontal beam focal spot, an external sample stage with motorised x-y (y being the focusing direction) movements and manual z was used.

2.2.1 Raman data processing

Data acquisition and spectra elaboration was performed with LabSpec software. All spectra underwent background subtraction using a linear baseline with attach points at about ~300, ~700, ~800/850 and 1300 cm^{-1}. The trend of the background, in particular before 300 cm^{-1} required adding further attaching points, which introduced some fictive signals in these areas that were not taken into account. Representative raw Raman spectra prior to background subtraction are reported in Fig 2.

Attribution of crystalline phases was made upon comparison with literature data and on-line databases (University of Parma 2009; Lafuente et al. 2015). The decomposition of the stretching and bending massifs of silica in its vibrational components followed the model proposed by Robinet et al. for lead-alkali glass (Robinet et al. 2008). We chose to apply this model in place of the Q_n components model proposed and defined by Colomban for the study of glassy silicate materials (Colomban 2003, Colomban 2005, Colomban et al. 2006a, Colomban et al. 2006b) which is generally used in literature (Ricciardi 2008, Tournié 2009, Ricciardi et al. 2009b, Kirmizi et al. 2010a, De Ferri et al. 2012, Caggiani et al. 2014). The model proposed by Robinet et al. is slightly more refined and it allows obtaining compositional data on lead, silica and alkali (alkaline+alkaline earth metals) contents, which we were interested in comparing with XRF quantitative results and whose results will be discussed in more detail in a forthcoming paper (Fenoglio et al. forthcoming).

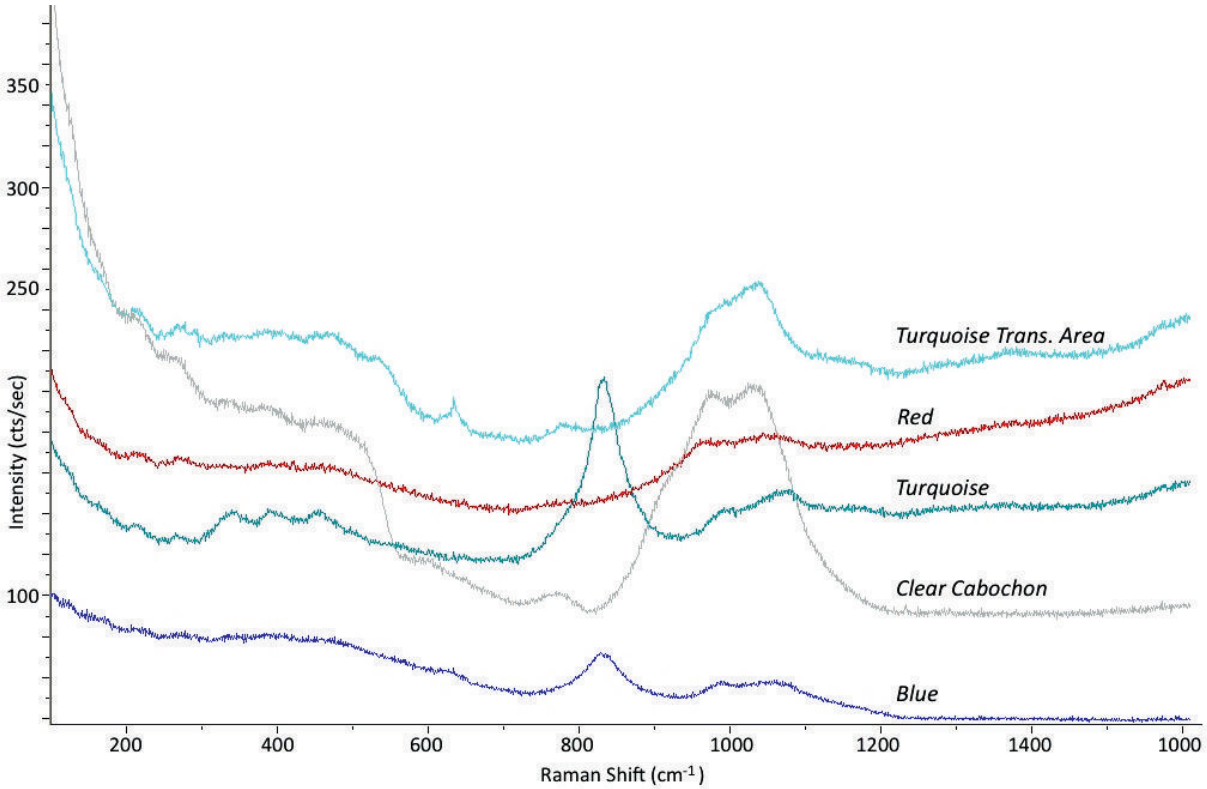

Fig. 2: Examples of raw Raman spectra obtained on K 4195 glassy materials.

2.2.2 Raman spectroscopy on glass

The spectrum obtained from a vitreous silicate-based material is a fingerprint of the glass structure and it is related to its composition and thermal history. Information on the matrix typology can be obtained comparing the spectra shape of the investigated glass with reference spectra of glass families as described in literature (Colomban et al. 2006a, Robinet et al. 2006, Robinet et al. 2008). The spectrum may contain crystalline phases that produce signals that need to be recognised and separated from the silica network fingerprint. Crystalline phases are generally associated to unreacted raw ingredients, opacifying or colouring agents, and produce sharp signals whose identification is based on comparison with literature or with on-line spectral database (University of Parma 2009, Lafuente et al. 2015).

Raman spectra of silicate glasses are instead characterised by two main massifs at about 300–600 cm^{-1} and 900–1300 cm^{-1}: the first corresponds to the convolution of Si-O-Si bending vibrations of the polymerised structure, and the second to Si-O stretching vibrations of depolymerised silicate species (Mysen et al. 1980, Mc Millan 1984, Robinet et al. 2006). The interpretation of the different vibrational components follows the model derived from the study of crystalline silicates. The tetrahedral structures are classified on the base of their structural units, which are identified with the number of Non-Bridging Oxygens (NBOs) and thus referred as Q_n, where n=0 for isolated tetrahedrons and n=4 for pure silica. For silica glasses the Q_n model indicates a total of five components for each massif, excluding that extra-bands can belong to the silicate network.

Specific assignments to glass families and more detailed information on the matrix require extracting specific Raman parameters: the wavelength shift and area of the bending and stretching regions, δ_{max} and A_{500}, ν_{max} and A_{1000} respectively. The ratio between A_{500} and A_{1000} is known as Polymerisation Index I_p and according to previous studies it is: a) correlated to the structure of the Si-O network and its polymerization degree; b) influenced by the nature and quantity of the modifiers and by the production techniques applied (Colomban 2003, Colomban 2005); c) correlated to the melting and working temperature, thus providing information on the production processes undergone by the studied object (Colomban 2003). For what concerns the maxima of the massifs, the shift of the ν_{max} is mostly related to the mass of modifiers' cations, while the δ_{max} origins from their ion charge, which involves changes in the Si-O angles (Kirmizi et al. 2010a).

2.3 Colour measurement

Colour measurements have been carried out by a Vis-spectrometer (Zeiss PDA Vis spectrometer, type MCS621 VIS II) coupled with a stereo zoom microscope (Zeiss SteREO Discovery V8 stereo microscope with 8x manual zoom). A more detailed description of the device used can be found elsewhere (Röhrs and Stehr 2014).

An external light source has to be used to illuminate the object surface. A cold light source with swan-neck light gui-

des (SCHOTT KL 1500 LCD with a Phillips 15 V, 150 W halogen cold light illuminant) was used. The illumination of the sample area can be adapted to be at 45° to the surface normal. The fibre optic of the light guides can be attached to the microscopic stand of the zoom microscope. This ensures that the illumination conditions remain identical when the microscope is moved relative to the object to focus onto the surface studied.

The diffuse reflected light passes through the zoom microscope and is guided to the spectrometer via an interface (manufactured by A.S. & Co Munich, Germany), which is fitted on the camera adapter and couples the microscope with the optical fibre.

The size and shape of the selected area on the object surface depends on the size and shape of the aperture in the interface and the magnification factor of the microscope.

Documentation of the selected area is possible with a digital camera. For the measurement of the enamels no pinhole was inserted into the microscope-spectrometer interface resulting in a selected area for the measurements with a diameter of approx. 0.4 mm at a zoom factor of 5.

The results of the colour measurements are presented as point in the CIELab colour space. The variable L gives the lightness of the colour. The projection into the a/b–plane represents the hue of the colour by their relative position to the a and b aches; the further a point is away from the origin of the coordinate system the stronger is the saturation of the colour.

Measurements on early enamels from Limoges and Rhenish / Mosan area have been carried out and can serve as references for the new measurements on the K 4195. The objects, which have been tested are: Book cover (KGM inv. no. 1908,38), Limoges 4. Quarter 12th c. AD; a Book cover (KGM inv. no. W-1974,59), Limoges, 1. Quarter 13th c. AD; Ornament (KGM inv. no. W-1984,25), Treves around 1230 AD and the so called Tower-Reliquary (Hessisches Landesmuseum Darmstadt inv. no. Kg 54:239), Cologne, 1180/90.

3 RESULTS AND DISCUSSION

3.1 Micro-XRF ANALYSES

3.1.1 Metal

Micro-XRF analysis performed on the exposed metal areas of the incense holder indicates a rather pure copper with traces of lead and iron, a composition which would be compatible with an original medieval artwork (England 1986, Biron et al. 1996). Gilded areas contain gold and mercury, the presence of the last element suggesting an amalgam gilding (Anheuser 1997), which has been used traditionally in the medieval Limoges. However, this gilding typology was widely used up to mid-19th century (Arminjon and Bilimoff 1998), and may still have been used later, particularly by smaller workshops. The enamelling would require a higher temperature than the process of the amalgam gilding. Over firing of a gilding during a re-enamelling process might lead to damage and delamination of the gilding as it has been observed on silver objects (van Bellegem et al. 2008) and any polishing of the enamels would have erased the gilding. Therefore, it is expected that the gilding has been performed after the enamelling.

3.1.2 Enamels

For what concerns the glass materials, XRF spectra were collected on all colour shades of enamels present on the artwork, that is blue, turquoise and red, and on the stones applied on the lid of the incense-holder. Attention was given to analyse the enamel in clean areas.

According to our results, all enamels applied on the object contain lead and arsenic, which would suggest lead arsenate as the opacifier. The use of this opacifier is considered an indicator of *en style de Limoges* artefacts produced during the 19th-20th centuries (Biron et al. 1996, Röhrs and Stege 2004). The enamels contain low amounts of Fe_2O_3 and TiO_2, Al_2O_3 being under the quantification limit, indicating a pure source of raw materials. CaO contents are about 1.5-2.0 wt%. K_2O contents are quite high, about 6-10 wt%. Considering that in all data the dark matrix is about 10 wt%, the presence of Na_2O is rather possible, suggesting a mixed alkali flux.

The blue enamel contains about 20 wt% PbO, 5 wt% As_2O_3, 7-8 wt% K_2O and 1.4 wt% CoO as colouring agent. BaO contents around 0.1 wt% appear to be connected to this enamel colour, such as NiO, which is most likely related to the presence of CoO.

The turquoise enamel indicates similar contents: 19-21 wt% PbO, 6-8 wt% As_2O_3 and 9 wt% K_2O. The enamel contains about 3-4 wt% CuO, considered to be the colouring agent. The presence of SnO_2, ranging from 1.5 to 4 wt%, can be explained as a necessary ingredient to obtain the turquoise colour in a lead-rich matrix, which would otherwise be green. According to literature, the addition of tin to the matrix would induce a shift towards blue, an effect also obtained with boron addition (Lehnhäuser 1959).

The red enamel shows relevant contents of iron and copper, both about 2.5 wt%, suggesting the presence of cuprite and/or hematite as colourants and opacifiers. Iron was generally introduced as reducing agent in order to facilitate the reduction of copper ions to cuprite, but in this case it could be present as hematite and contribute to the colour and opacification. The As_2O_3 content is much lower, around 0.5 wt%, while contents similar to the previous colours are observed for the other elements: about 24 wt% PbO and 7 wt% K_2O.

The analysis of the cabochons indicates that both are lead-rich glasses, with PbO contents around 30-40 wt%. Both glasses contains about 0.5 wt% Fe_2O_3, while the green one contains a higher CuO content, about 0.9 wt%, which is most likely the colouring agent.

Tab. 1: Quantitative µ-XRF results expressed in wt% (nd = not detected)

Measure	Al_2O_3	SiO_2	K_2O	CaO	TiO_2	MnO	Fe_2O_3	CoO	NiO	CuO	ZnO	As_2O_3	SnO_2	PbO	BaO	SUM
Blue	<1.2	52	7.5	2.2	0.030	0.24	0.12	1.3	0.05	0.05	0.007	4.8	nd	19.7	0.14	87
Turquoise	<1.3	47	9	1.7	0.020	0.05	0.10	nd	nd	3.7	0.023	7.1	2.5	20.1	nd	91
Red	nd	43	7.7	2.1	0.020	0.05	2.40	nd	nd	2.60	0.400	0.4	nd	23.8	nd	82
Clear Cabochon	<1.3	45	5.9	2.9	0.100	0.10	0.61	nd	nd	0.33	0.036	0.0	nd	40.0	nd	92

3.2 RAMAN ANALYSIS

3.2.1 Crystalline Phases

The presence of an arsenate compound acting as opacifier, proposed upon XRF results, was confirmed in both blue and turquoise enamel by a strong signal at 830 cm^{-1} (Fig. 3). This signal is characteristic of As-O stretching vibrations of the AsO_4^{3-}-ion, which are generally revealed between 810 and 850 cm^{-1} in Ca/Pb arsenate compounds (Caggiani et al. 2014). The identification of the specific arsenate compound is not straightforward. The literature review allowed underlying that some authors use the term "lead arsenate" in reference to a phase identified with the main peak at 813 cm^{-1} (Van Pevenage et al. 2014) and 820 cm^{-1} (Kirmizi et al. 2010b). Colomban (2012) uses the general term "arsenate white", most likely meaning lead arsenate, for a phase characterised with peaks at about 815-825 cm^{-1}. Other authors are more cautious and refer identifying a general Ca/Pb arsenate compound thanks to the strong narrow peak at 825 cm^{-1} (Ricciardi 2009, Tournié 2012). Caggiani et al. (2014) indicate detecting a distinctive shift of the peak in two different sets of objects, varying from 815-825 to 805-810 cm^{-1}, suggesting the presence of two arsenate phases. The signal observed in the enamel of K 4195 appears to be positioned at slightly higher wavelengths than reported in the literature. However, the same peak at 830 cm^{-1}, was also observed on Raman spectra collected on laboratory samples opacified with arsenate in a lead rich matrix.

The blue enamel appears to be very homogenous with no noticeable grains within the matrix, suggesting that a very fine powder was used for its production (Fig. 4a). On the contrary, a more detailed observation of the turquoise enamel allowed observing the presence of transparent areas dispersed within the enamel, possibly a clear glass surrounding homogenous grains of turquoise opaque glass (Fig. 4b). In some cases the clear glass was bearing white crystalline clusters, which could be identified as cassiterite, tin dioxide, thanks to the doublet at about 635 and 775 cm^{-1} (Fig. 3).

The Raman spectra collected on the red enamel contained only little Raman signal and more spectral noise compared to the other spectra. Neither lead arsenate signals nor a clear signature for the red colouring agent was identified (Fig. 3). Two small peaks at 215 and 270 cm^{-1} seemed to be indicative of a phase presence. However, these signals were observed in all spectra collected on K4145 and could not be assigned to any specific phase. The presence of a weak signal at about 490 cm^{-1} together with a signal at 215 cm^{-1} would suggest the presence of hematite, though this does not exclude the presence of cuprite within the matrix.

The clear bead did not show the presence of any crystalline compound, the spectra only showing the silica-matrix massifs (Fig. 3).

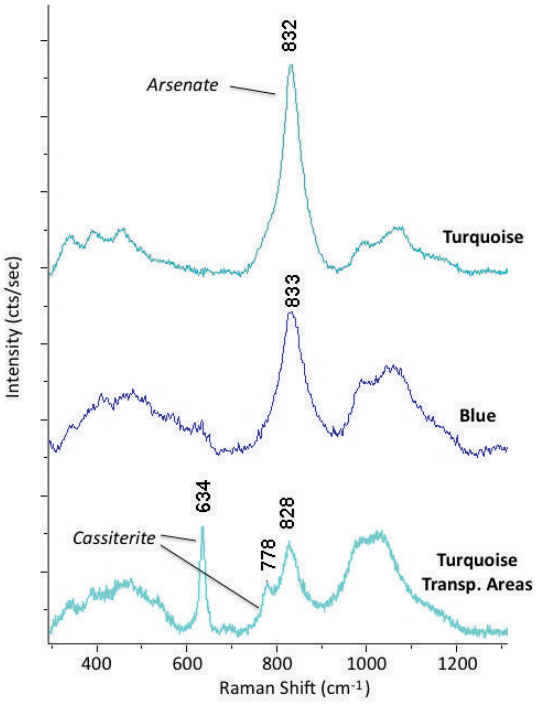

Fig. 3: Raman spectra of blue and turquoise opaque enamel indicating AsO_4^{3-}-ion signal, white cluster in the clear transparent area of the turquoise revealing Cassiterite doublets.

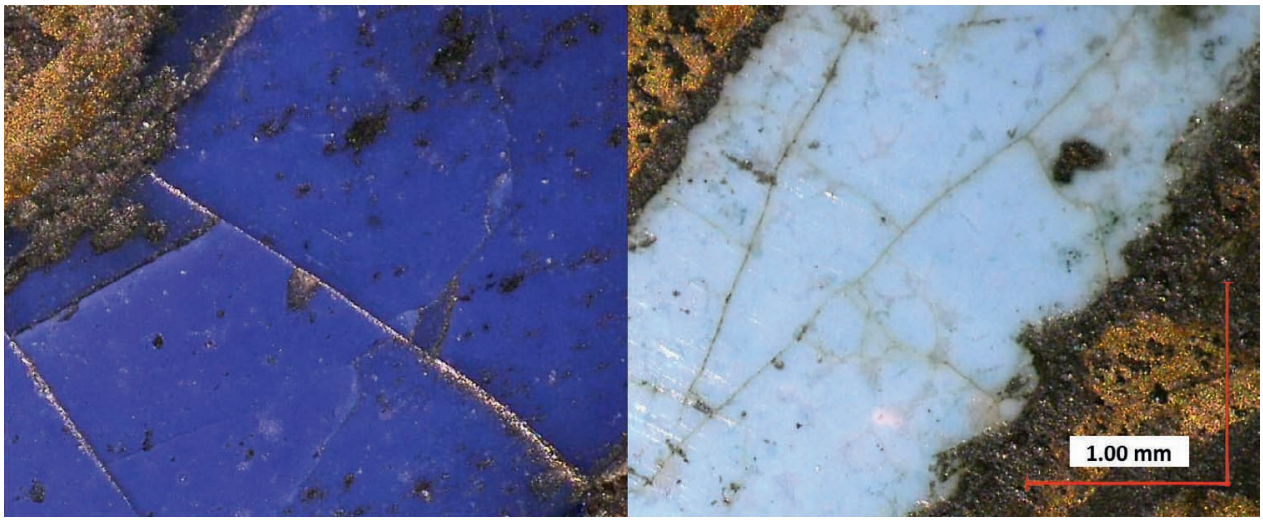

Fig. 4: Microphotography of the blue (left) and turquoise enamel (right). The clear glass surrounding the opaque turquoise glass is visible, and some very fine blue grains can also be observed. These are most likely a contamination from the blue powder used for the blue enamel during the fabrication process and confirm its very fine grinding.

3.2.2 Glass matrix

The shape of the stretching and bending regions of silica in the Raman spectra indicates a lead-bearing glass matrix for all enamels (Fig. 5). The maximum of the stretching region (ν_{max}) and the whole massif of stretching signals is positioned towards lower wavelengths compared to alkali-silica glasses.

Nevertheless, variations in the stretching region can be observed: The transparent bead and transparent glass of turquoise enamels are similar in the stretching region shape, for what concerns the wavenumber and intensity of the maximum. The spectra are centred at lower wavelengths, ν_{max} being 1030 cm^{-1} for the clear bead and the clear glass in the turquoise. Substantially different are the blue and turquoise opaque enamels, with doublets at about 990 and 1060-1070 cm^{-1}, the second one being the most intense.

Different again is the red enamel, with ν_{max} at about 965 cm^{-1}.

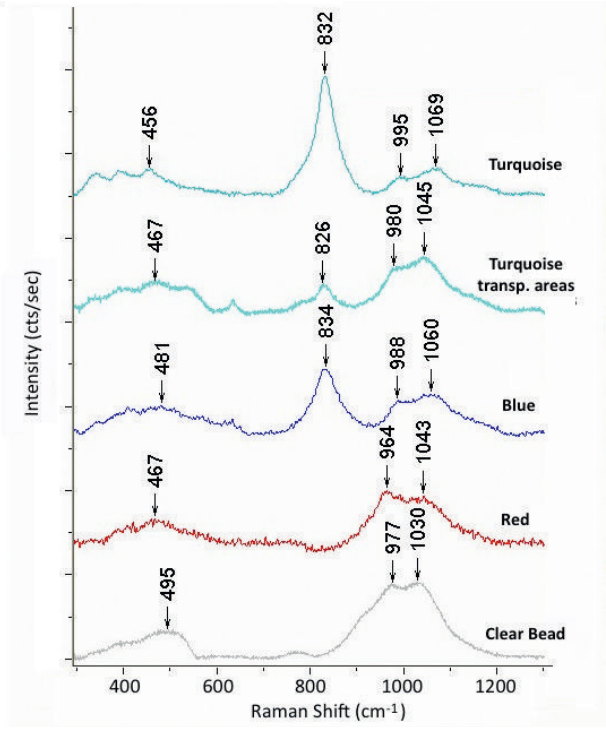

Fig. 5: Representative spectra of the enamels (blue, turquoise opaque and clear areas, red) and the clear bead.

3.2.3 Raman parameters of bending and stretching regions in spectra of glass

In order to obtain detailed information on the glass matrix, the spectra were decomposed and parameters were extracted from the Raman spectra. These comprehend the wavelength of the bending and stretching regions, δ_{max} and ν_{max}, and the area of the corresponding massifs, whose ratio (A_{500}/A_{1000}) gives the polymerisation index I_p. Average data are shown in Tab. 2 and plots of obtained parameters are presented in Fig. 6 and Fig. 7, together with clusters associated to specific compositional information derived from literature. In particular, in Fig. 6 the bending and stretching maxima are correlated to shifts induced by the content of glass modifiers (Robinet et al. 2006, Robinet et al. 2008, Ricciardi et al. 2009a, Kirmizi et al. 2010a, Colomban et al. 2012). In Fig. 7 data is compared to clusters associated to *Glass* Families as defined in Colomban studies on glassy silicates (Colomban et al. 2006a) together with further information on alkali and lead-induced ν_{max} shifts (Robinet et al. 2006, Robinet et al. 2008).

Plot of δ_{max} against ν_{max} (Fig. 6) suggests a high PbO matrix for the red enamel. Blue and turquoise enamels are close to the Na_2O low CaO group (Ricciardi et al. 2009a, Kirmizi et al. 2010a) or to alkali lead glasses. The clear cabochon and clear transparent glass of the turquoise fall in an intermediate position between red and blue/turquoise enamels.

The plot of the ν_{max} and I_p (Fig, 7) indicates a similar situation. According to Glass Families subdivision (Colom-

ban et al. 2006a) the red enamel belongs to the PbO rich group and the clear bead and clear glass of the turquoise fall together with the PbO+Na_2O group. The blue and turquoise enamel are again close to the Na_2O group, in particular because of the relevant I_p, while information on ν_{max} shifts on alkali and lead bearing matrices (Robinet et al. 2006, Robinet et al. 2008) would rather suggest an alkali lead matrix. As better explained in the following paragraphs, the interpretation of the Raman data is not straightforward. The XRF data indicates a rather high K_2O content, which has not been discussed in previous Raman literature and data obtained on blue and turquoise enamel is probably affected by a relevant overestimation of the I_p, which would move its position on the plot towards the PbO+Na_2O group.

Remarks on the role of baseline subtraction and crystalline phases in the calculation of I_P values

As reported in the "Experimental" section, all collected spectra present a relevant contribution by spectral background in the low-wavenumber region (Fig. 2). The background subtraction in this region can induce a modification of the I_p ratio, and previous works already suggested considering this parameter in a relative rather than absolute way (Ricciardi et al. 2009b, Kirmizi et al. 2010b). According to our experience, shifting the baseline attaching point close to the massif at 500 cm^{-1} to the positions 200, 240 or 300 cm^{-1} (hereafter referred as Bk_{200}, Bk_{240}, Bk_{300}) may produce relevant I_p variations. In particular, results on reference materials indicate that alkali silicate matrices undergo an I_p reduction of about 0.2 when moving the attaching point from Bk_{240} to Bk_{300}. Similar results were observed for low-Ca Pb-containing glasses, while high lead and soda-lead did not present relevant variations. Data obtained using Bk_{240} seems falling in the correct *Glass Family* cluster, however this baseline could not be applied because of the presence of a couple of parasite peaks at about 215 cm^{-1} and 270 cm^{-1} in all collected spectra. Considering this information, Raman features obtained on Corning glasses A and B applying Bk_{300} were also plotted on the graphs to give an indication of I_p shifts due to spectra processing.

A further point of discussion is that all previous works on Raman spectroscopy applied to glassy matrices underline the necessity to obtain "good quality spectra" to produce reliable data. In some cases specific colours (i.e. yellow) were completely excluded, as it was not possible to avoid signals from the crystalline phases (Kirmizi et al. 2010a). Indeed, when the presence of crystalline compounds cannot be avoided in the spectrum and their content is relevant, the removal of their contributions is a further step that can induce errors in the I_p calculation.

In the specific case of incense holder K 4195, the presence of a strong lead arsenate signal in the blue and turquoise opaque enamel also concealed the presence, position and intensity of the weak bands at about 800 cm^{-1} related to the Si-O-Si network. In a minor way, it probably also affected the intensity of the bands at 922 cm^{-1}, 950 cm^{-1} and 990 cm^{-1} related to Q_2 Si-O signals. In general, we suppose that spectra collected on the blue and turquoise are susceptible of an underestimation of the 922 cm^{-1} and 950 cm^{-1} components and as a consequence, an overestimation of the I_p, and possibly of ν_{max}.

Comparison of Raman compositional information with XRF data

When comparing the assumptions made on the matrix typology upon Raman to XRF data, a principal difference is the K_2O content, as Raman results tend to indicate a Na_2O dominated flux with variable PbO contents and XRF analysis indicates the presence of a relevant K_2O content, about 6-10 wt%, in all enamels and in the cabochons. When working on heterogeneous material, differences are to be expected between XRF and Raman results. XRF analysis produces an average data on the composition of the analysed volume, including the glass matrix and eventual crystalline phases. On the contrary, when performing Raman analysis of the matrix, particular attention is given to collect spectra excluding the crystalline phases, as their signals can interfere with the study of the silica matrix signals. However, according to the author opinion, the different K_2O contents do not present a real divergence between Raman and XRF data upon the type of flux. In the first place, XRF data indicates a dark matrix around 10 wt%, thus suggesting the presence of Na_2O. In second place, as this specific composition, Pb-silica glass with mixed alkali flux and low CaO, is not discussed in literature, the behaviour of its Raman parameters still has to be better determined, and it does not exclude a superposition with other glass families. In third place, for what concerns the blue and turquoise enamels, it has been described above that we expect an overestimation of the I_p, and possibly of the ν_{max}, which would move these data towards Raman features owned by the clear bead and clear glass of the turquoise.

In general, Raman features confirm the reduced content of CaO, while the information on glass modifiers, apart from the presence of Na_2O, is less clear. Considering literature, a shift of ν_{max} towards lower wavelengths suggests increasing contents of PbO or K_2O, while an increase in CaO induces a shift of δ_{max} towards higher wavelengths. The information on K_2O content provided by XRF analysis let arise a relevant question about the interpretation of the shift along the ν_{max}. Our data suggest a difficulty in discriminating shifts produced by PbO presence in a Na_2O or mixed alkali matrix, which would require further studies.

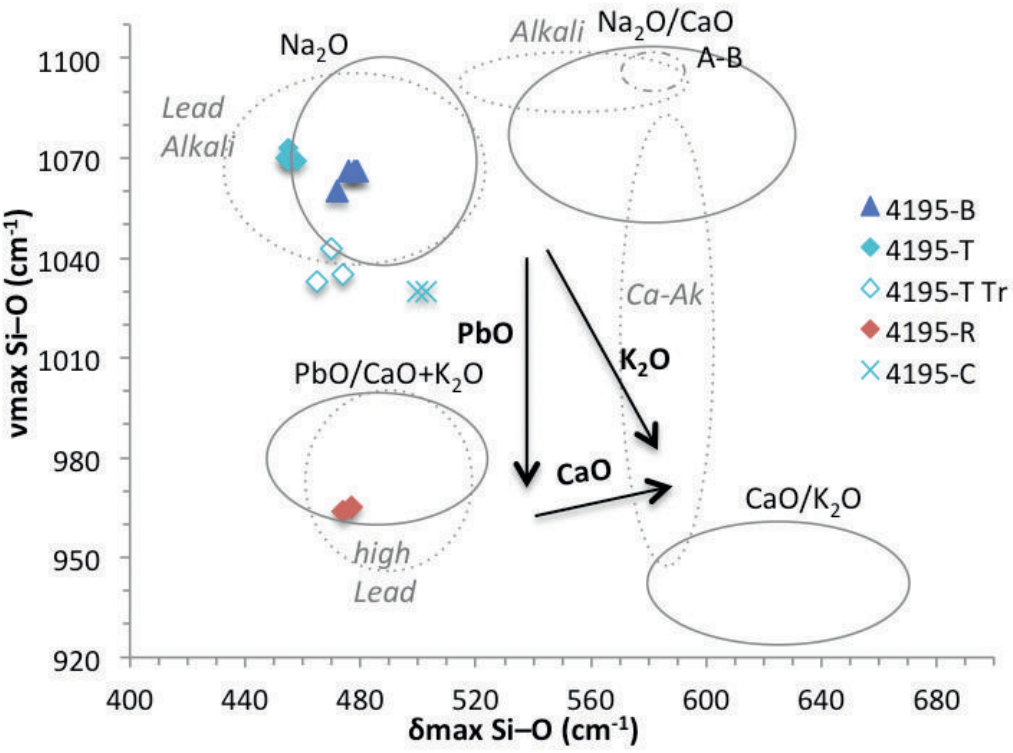

Fig. 6: Plot of Si-O bending *versus* Si-O stretching maxima. Compositional clusters are indicated according to literature: continuous line (Ricciardi et al. 2009; Kirmizi et al. 2010a; Colomban et al. 2012); dotted line (Robinet et al. 2006; Robinet et al. 2008). Arrows are from (Colomban 2013). Data obtained on Corning glasses A and B are indicated by the circle with dotted-dashed line.

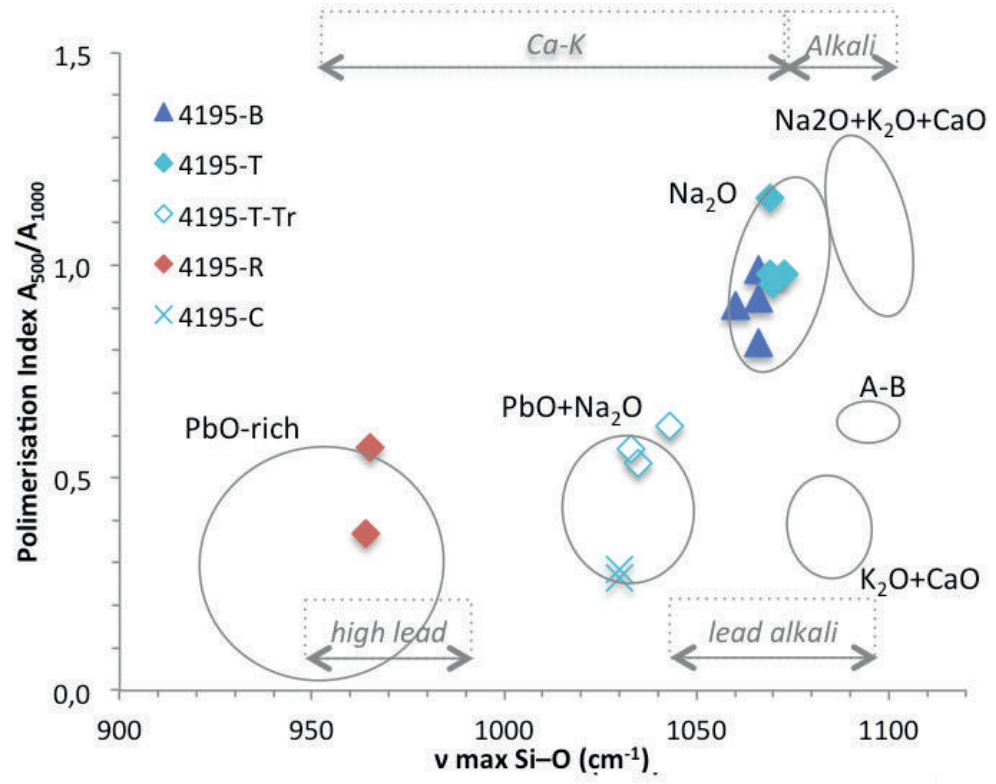

Fig. 7: Plot of Si-O stretching maxima *versus* I_p. Compositional clusters are indicated according to literature: continuous line (Ricciardi et al. 2009), dotted line (Robinet et al. 2006; Robinet et al. 2008). Data obtained on Corning glasses A and B are indicated by the circle.

Tab. 2: Average Raman features calculated upon deconvolution of the spectra with Bk_{300}.

	δ_{max}	ν_{max}	I_P
Blue	476	1065	0.9
st.dev.	*3*	*3*	*0.1*
Turquoise	456	1070	1.1
st.dev.	*2*	*2*	*0.1*
Turq. Clear	470	1037	0.6
st.dev.	*5*	*5*	*0.1*
Red	476	965	0.5
st.dev.	*2*	*1*	*0.1*
Clear bead	502	1030	0.3
st.dev.	*2*	*0*	*0.0*

3.3 Colour measurements

The colours red, blue and turquoise of the incense holder K 4195 have been measured and compared with measurements from a series of medieval Limoges and Rhenish / Mosan enamels. For comparison the measurements results have been plotted in a graph representing the colour values a* and b*. The corresponding colours, which are perceived by the human eye, are indicated by the labels in the rectangular shapes (Fig. 8). The measurement points of the incense holder do not fall together with the group of the medieval enamels. The turquoise data points have lower a* values compared to the reference group. The data points from the red and the blue of K 4195 are further away from the origin of the graph. Especially, the blue of K 4195 is at much higher a* and lower b* values and was the colour which arouse interest in this objects for further studies because of the slight reddish hue of the blue.

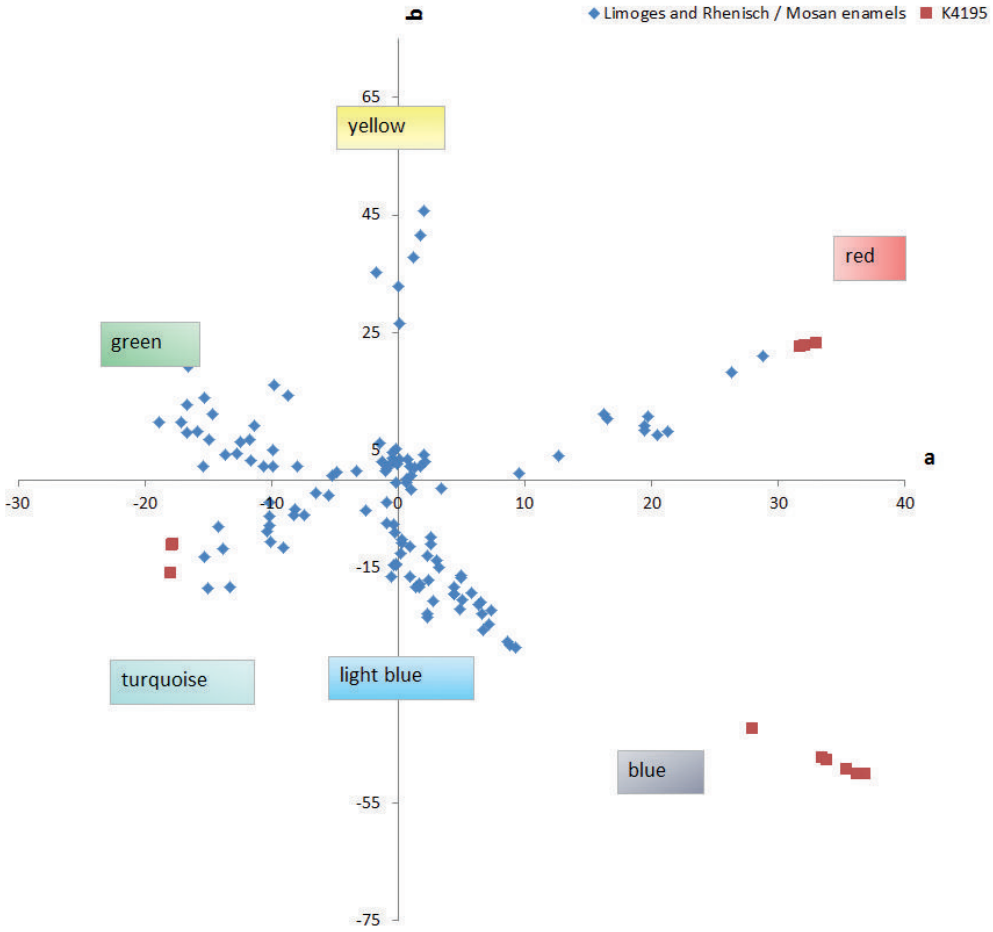

Fig. 8: Plot of the colour measurements projected on the a*/b* plane which allows to differentiate the hues of the colours.

4 Conclusions

In the present work a non-invasive multi-technique approach, based on μ-XRF, μ-Raman micro-spectroscopy and colour measurements, was applied to verify the compatibility of incense holder K 4195 with a traditional medieval Limoges manufacturing techniques and to obtain information on the composition of the enamels and the colouring and opacifying agents.

The conjoint application of μ-XRF and μ-Raman spectroscopy allowed characterising the crystalline phases and an in-depth study of the glassy matrix. Information provided by μ-Raman investigation of the matrix is complementary to μ-XRF results. Point measurements by μ-XRF, even at this micro-scale with a spot size of 100 μm always gives average elemental information on the analysed area, including both crystalline phases and the glass matrix. The μ-Raman investigation uses a spot size on the order of several μm, thus generally enabling to probe these phases separately.

In the case of incense holder K 4195 μ-Raman analysis allowed differentiating glass typologies used for the enamelling, suggesting that they belong to Glass Families 5 and 7, i.e Na_2O+PbO and high PbO. In the case of the turquoise enamel two different glasses were found in the same colour.

However, the interpretation of the glass families still needs some more methodological work. According to literature, Raman parameters allow differentiating compositional clusters associated to modifiers presence. No detailed information was however available in literature on the Raman parameters associated to this specific composition, which is a high-lead low-calcium mixed alkali silica glass. Furthermore, the influence of compositional additions that are typical for enamels has not been considered by other authors. Compared to glass and transparent glazes used in literature to define compositional clusters, the enamels of incense holder K 4195 have a higher content of opacifiers (here e.g. arsenates) and colouring ions (as copper). Their role on Raman signal, in particular the arsenates presence, has not been discussed in detail, suggesting that further studies are needed.

In conclusion, according to the analytical results obtained in this study, the compositions of the enamels of the incense holder K4195 which were analysed are not consistent with an original medieval Limoges artwork. Particularly, the higher lead values and the use of an arsenate-based opacifier are features typical of a 19th-20th century production.

The colour measurements did indicate discrepancies between the enamels of the incense holder and genuine medieval é*mail champlevé*. The most significant colour difference was found in the blue enamels although the same colouring ion (i.e. cobalt) has been used. This result is interesting as it indicates that certain glass matrices are shifting colours in such a way, that it can be picked up by eye and via Vis-spectroscopy.

The analysis of the metal and the amalgam gilding did not allow obtaining further indication for the production date of the object. The materials used are not strictly indicative for a certain period (England 1986, Biron et al. 1996). However, it is likely that the gilding is post medieval too, as it had most likely been applied after the enamelling, since polishing the enamels surface after its firing would have removed or damaged the remaining gilding.

Nonetheless, there are several arguments against the attribution of the *Weihrauchschiffchen* of the Berlin *Kunstgewerbemuseum* being, as a whole, a reproduction from the 19th century.

The characteristic construction of the object, the extensive traces of corrosion and use, as well as the stylistically uncritical ornamental work and the less elaborated way of their execution indicate the contrary.

Two stylistic and technical closely related incense holders in Paris define the art historical context for the provenance of the Berlin *Weihrauchschiffchen* to the Limoges ateliers of the 13th century, i.e. in the *Musée du Louvre* (Gauthier et al. 2011, VI C, n° 6) and the *Musée de Cluny* (Rupin 1890, Fig. 605). The object could therefore be a *pastiche*, i.e. an original medieval base re-enamelled with a 'modern enamel'.

The incense holder K 4195 was assigned to the Berlin *Kunstgewerbemuseum* from the *Königliche Kunstkammer* (Royal Art chamber) in 1875. Almost two decades before, in 1856, the object was purchased by the *Kunstkammer* from the Berlin art dealer Friedrich Meyer. Already at that time, the object had been at large in this today's condition, as it can be read in the description of the object in the inventory of acquisitions. Although the contemporary alteration of the enamel had been deliberately understated, the inventory entry testifies that the enamels had been partly renewed: *„Emaillen theilweise erneuert"*

The documented collection historic circumstances therefore allow dating this remarkable early extensive re-enameling of a medieval Limoges artwork with industrial raw materials to the period before 1856.

Acknowledgements

For the help with reference material we owe thanks to Manfred Torge and Ines Feldmann from the *Fachbereich 4.2 "Materialien und Luftschadstoffe" of the Bundesanstalt für Materialforschung und –prüfung* (BAM) Berlin.

We are also most grateful to Angelo Agostino for providing WinAxil software and for his support and recommendations in producing XRF quantitative data.

We thank the *Förderkreis des Rathgen-Forschungslabors e.V.* for the financial support through the Rathgen Heritage Scholarship 2015.

Finally, we would like to thank the IPERION-CH project funded by the European Commission, H2020-INFRAIA-2014-2015, under Grant No. 654028 for providing an additional possibility to consult analytical data via the access platform ARCHLAB.

References

A. Agostino, M. Aceto, S. Castronovo (2010): Autenticazione di opere di oreficeria limosini mediante analisi di Fluorescenza di Raggi X e analisi multivariata. La "Collection Larcade," In *Proceedings of Congresso tematico AlAR09 - Riflessioni e trasparenze, diagnosi e conservazione di opere e manufatti vetrosi (Ravennna, 24-26 febbraio 2009)*, Patròn Editore.

K. Anheuser (1997): The practice and characterization of historic fire-gilding techniques, *The Journal of the Minerals, Metals & Materials Society*, 49, 58–62.

C. Arminjon, M. Bilimoff (1998): *L'art du metal; vocaboulaire technique*, Editions du Patrimoine, Paris.

M. van Bellegem, S. Röhrs, B- McLeod (2008): A Spanish Medieval altar "set": new investigation and assessment of its date and manufacture, *The British Museum Technical Research Bulletin*, Volume 2, 67–76.

I. Biron, P. Dandridge, M. T. Wypyski (1996): Techniques and materials in Limoges enamels, In *Enamels of Limoges: 1100-1350.* (ed. J. O' Neill), 48–62, 446–8, Metropolitan Museum of Art, New York.

I. Biron (2015): Émaux sur metal du IXe au XIXe siècle. Histoire, technique et matériaux., Ed. Faton.

J. Braun (1932): Das christliche Altargerät in seinem Sein und in seiner Entwicklung, München.

R. H. Brill (1999): Chemical analyses of early glasses: Volume 1 (tables) and 2 (catalogue), Corning Museum of Glass, New York.

M. C. Caggiani, C. Valotteau, P. Colomban (2014): Inside the glassmaker technology: search of Raman criteria to discriminate between EmileGallé and Philippe-Joseph Brocard enamels and pigment signatures, *Journal of Raman Spectroscopy* (45), 456–64.

P. Colomban (2003): Polymerization degree and Raman identification of ancient glasses used for jewelry, ceramic enamels and mosaics, *Journal of Non-Crystalline Solids*, 323 (1-3), 180–7.

P. Colomban (2005): Non-Destructive Determination of the Structure and Composition of Glazes by Raman Spectroscopy, *Journal of American Ceramic Society* (88), 390–5.

P. Colomban, A.Tournié, L. Bellot-Gurlet (2006a): Raman identification of glassy silicates used in ceramics, glass and jewellery: a tentative differentiation guide, *Journal of Raman Spectroscopy* (37), 841–52.

P. Colomban, M. P Etcheverry, M. Asquier, M. Bounichou, A. Tournié (2006b): Raman identification of ancient stained glasses and their degree of deterioration, *Journal of Raman Spectroscopy*, 37(5), 614–26.

P. Colomban, A. Tournié, M. C. Caggiani, C. Paris (2012): Pigments and enamelling/gilding technology of Mamluk mosque lamps and bottle, Journalof Raman Spectroscopy(43), 1975–84.

P. Colomban (2013): The destructive/non-Destructive Identification of enameled pottery, glass artifacts and associated pigments—A Brief Overview, Arts, 2, 77–110.

P. England (1986): A technical investigation on Medieval Enamel, In *Catalogue of Medieval objects. Enamels and glasses* (eds. H. Swarzenski, and N. Netzer), xviii – xxvi, The Museum of Fine Arts, Boston.

P. Van Espen, P. Lemberge (2000): ED-XRF spectrum evaluation and quantitative analysis using multivariate and non-linear techniques, *Advanced X-Ray Journal*, 43, 560–9.

L. De Ferri, D. Bersani, A. Lorenzi, P. P. Lottici, G. Vezzalini, G. Simon (2012): Structural and vibrational characterization of medieval like glass samples, *Journal of Non-Crystalline Solids*, 358(4), 814–9.

I. Freestone (1991): Looking into glass, In *Science and the Past* (ed. S. G. E. Bowman), 37–57, British Museum Press, London.

M. M. Gauthier, É. Antoine, D. Gaborit-Chopin (2011): *Corpus des émaux méridionaux. Catalogue international de l'Œuvre de Limoges. Tome II: L'Apogée 1190–1215*, Ed. Musée du Louvre, Comité des travaux historiques et scientifiques.

B. Kirmizi, P. Colomban, B. Quette (2010a): On-site analysis of Chinese Cloisonn´e enamels from fifteenth to nineteenth centuries, *Journal of Raman Spectroscopy*(41), 780–90.

B. Kirmizi, P. Colomban, M. Blanc (2010b): On-site analysis of Limoges enamels from sixteenth to nineteenth centuries: an attempt to differentiate between genuine artefacts and copies, *Journal of Raman Spectroscopy*, 41(10), 1240–7.

D. Kötzsche (1975): Limousiner Metallarbeiten des Mittelalters aus dem Besitz des Kunstgewerbemuseums Berlin, Berlin.

B. Lafuente, R. T. Downs, H. Yang, N. Stone (2015): The power of databases: the RRUFF project, In *Highlights in Mineralogical Crystallography* (eds. T. Armbruster, and R. M. Danisi), 1–30, W. De Gruyter, Germany.

W. Lehnhäuser (1959): *Glasuren und ihre Farben* 3°-1973rd ed., Knapp, Dusseldorf.

P. Mc Millan (1984): Structural studies of silicate and melts - applications and limitations of Raman spectroscopy, *American Mineralogist*, 69, 622–44.

B. O. Mysen, D. Virgo, C. M. Scarfe (1980): Relations between the anionic structure and viscosity of silicate melts - a Raman spectroscopic study, *American Mineralogist*, 65, 690–710.

J. Van Pevenage, D. Lauwers, D. Herremans, E. Verhaeven, B. Vekemans, W. De Clercq, L. Vincze, L. Moensa, and P. Vandenabeeleb (2014): A combined spectroscopic study on Chinese porcelain containing ruan-cai colours, *Analytical Methods*(6), 387–94.

P. Ricciardi (2008): Raman spectroscopy for the non destructive characterization of ancient pottery, porcelains and mosaic glasses, *Plinius*, 34, 139–46.

P. Ricciardi, P. Colomban, A.Tournié, V. Milande (2009a): Nondestructive on-site identification of ancient glasses: genuine artefacts, embellished pieces or forgeries?, *Journal of Raman Spectroscopy* (40), 604–17.

P. Ricciardi, P. Colomban, A. Tournié, M. Macchiarola, N. Ayed (2009b): A non-invasive study of Roman Age mosaic glass tesserae by means of Raman spectroscopy, *Journal of Archaeological Science*, 36(11), 2551–9.

R. Richter (1994): Between original and imitation: four technical studies in basse-taille enameling and re-enameling of the Historicism period, *The Bulletin of the Cleveland Museum of Art*, 81(7), 223–51.

L. Robinet, C. Coupry, K. Eremin, C. Hall (2006): The use of Raman spectrometry to predict the stability of historic glasses, *Journal of Raman Spectroscopy*(37), 789–97.

L. Robinet, A. Bouquillon, J. Hartwig (2008): Correlations between Raman parameters and elemental composition in lead and lead alkali silicate glasses, *Journal of Raman Spectroscopy* (39), 618–26.

S. Röhrs, H. Stege (2004): Dating indicators for authenticity problems of Limoges painted enamels basing on material characterization, In *Neue Forschungen zum Maleremail aus Limoges - New researches on Limoges painted enamels* (eds. I. Musch, and H. Stege), 100–7, Herzog Anton Ulrich Museum, Barunschweig.

E. Rupin (1890): L'Œuvre de Limoges: ouvrage orné de 500 gravures, dont un grand nombre tirées hors texte, d'après les dessins et les photographies de l'auteur, Picard, Paris.

A. Tournié (2009): Analyse Raman sur site de verres et vitraux anciens: modélisation, procédure, lixiviation et caractérisation, Thèse Université Pierre et Marie Curie, Paris.

University of Parma (2009): Mineral Raman Database, URL: http://www.fis.unipr.it/phevix/ramandb.php.

B. Wagner, A. Nowak, E. Bulska, K. Hametner, D. Günther (2012): Critical assessment of the elemental composition of Corning archeological reference glasses by LA-ICP-MS., *Analytical and Bioanalytical Chemistry*, 402(4), 1667–77.

M. T. Wypyski (2000) Technical Appendix: Compositions of Enamels on the George Watch, *Metropolitan Museum Journal*, 35, 7.

Corresponding author:
Gaia Fenoglio (gaia.fenoglio@gmail.com)